

Onion-structured transition metal dichalcogenide nanoparticles by laser fabrication in liquids and atmospheres

Le Zhou(周乐), Hongwen Zhang(张洪文), Qian Zhao(赵倩), and Weiping Cai(蔡伟平)
Citation: Chin. Phys. B, 2022, 31 (**7**): 076106. DOI: 10.1088/1674-1056/ac539c
Journal homepage: http://cpb.iphy.ac.cn; http://iopscience.iop.org/cpb

What follows is a list of articles you may be interested in

Evolution of defects and deformation mechanisms in different tensile directions of solidified lamellar Ti-Al alloy

Yutao Liu(刘玉涛), Tinghong Gao(高廷红), Yue Gao(高越), Lianxin Li(李连欣), Min Tan(谭敏), Quan Xie(谢泉), Qian Chen(陈茜), Zean Tian(田泽安), Yongchao Liang(梁永超), and Bei Wang(王蓓)
Chin. Phys. B, 2022, 31 (**4**): 046105. DOI: 10.1088/1674-1056/ac1f0b

Formation of nano-twinned 3C-SiC grains in Fe-implanted 6H-SiC after 1500-℃ annealing

Zheng Han(韩铮), Xu Wang(王旭), Jiao Wang(王娇), Qing Liao(廖庆), and Bingsheng Li(李炳生)
Chin. Phys. B, 2021, 30 (**8**): 086107. DOI: 10.1088/1674-1056/abff43

Mechanical property and deformation mechanism of gold nanowire with non-uniform distribution of twinned boundaries: A molecular dynamics simulation study

Qi-Xin Xiao(肖启鑫), Zhao-Yang Hou(侯兆阳), Chang Li(李昌), and Yuan Niu(牛媛)
Chin. Phys. B, 2021, 30 (**5**): 056101. DOI: 10.1088/1674-1056/abd162

Understanding of surface pit formation mechanism of GaN grown in MOCVD based on local thermodynamic equilibrium assumption

Zhi-Yuan Gao(高志远), Xiao-Wei Xue(薛晓玮), Jiang-Jiang Li(李江江), Xun Wang(王勋), Yan-Hui Xing(邢艳辉), Bi-Feng Cui(崔碧峰), De-Shu Zou(邹德恕)
Chin. Phys. B, 2016, 25 (**6**): 066105. DOI: 10.1088/1674-1056/25/6/066105

Phase field modeling of the ring-banded spherulites of crystalline polymers: The role of thermal diffusion

Wang Xiao-Dong, Ouyang Jie, Su Jin, Zhou Wen
Chin. Phys. B, 2014, 23 (**12**): 126103. DOI: 10.1088/1674-1056/23/12/126103

TOPICAL REVIEW — Laser and plasma assisted synthesis of advanced nanomaterials in liquids

Onion-structured transition metal dichalcogenide nanoparticles by laser fabrication in liquids and atmospheres

Le Zhou(周乐), Hongwen Zhang(张洪文), Qian Zhao(赵倩), and Weiping Cai(蔡伟平)[†]

Key Laboratory of Materials Physics, Anhui Key Laboratory of Nanomaterials and Nanotechnology, Institute of Solid State Physics, HFIPS, Chinese Academy of Sciences, Hefei 230031, *China*

(Received 30 November 2021; revised manuscript received 28 December 2021; accepted manuscript online 10 February 2022)

Since the discovery of transition metal dichalcogenide (TMDC) nanoparticles (NPs) with the onion-like structure, many efforts have been made to develop their fabrication methods. Laser fabrication (LF) is one of the most promising methods to prepare onion-structured TMDC (or OS-TMDC) NPs due to its green, flexible, and scalable syntheses. In this mini-review article, we systematically introduce various laser-induced OS-TMDC (especially the OS-MoS_2) NPs, their formation mechanism, properties, and applications. The preparation routes mainly include laser ablation in liquids and atmospheres, and laser irradiation in liquids. The various formation mechanisms are then introduced based on the different preparation routes, to describe the formations of the corresponding OS-NPs. Finally, some interesting properties and novel applications of these NPs are briefly demonstrated, and a short outlook is also given. This review could help to understand the progress of the laser-induced OS-TMDC NPs and their applications.

Keywords: transition metal dichalcogenide nanoparticles, onion-like structure, laser fabrication in liquids, formation mechanism

PACS: 61.46.Df, 61.48.–c, 52.38.Mf **DOI:** 10.1088/1674-1056/ac539c

1. Introduction

Transition metal dichalcogenides (TMDCs), as the important semiconductors with the formula MX_2 (M = Mo, W, Ta, *etc.*; X = S, Se, Te, *etc.*), have attracted much attention due to their excellent optical, electronic, mechanical, thermal and chemical properties,[1,2] and extensive applications[3] in the fields such as photo/electrocatalysis,[4] sensing,[5] biomedicine,[6] battery,[7] and so on.[8,9] Generally, TMDC materials are composed of strongly chemical bonded layers with weak interlayer attraction held by van der Waals interactions. They tend to be exfoliated or prepared into two-dimensional (2D) nanosheets because of their intrinsic layered crystal structure. A lot of research, which lasted for decades, are mainly focused on these 2D nanosheets. In fact, those TMDCs could concentrically 'roll up' their layers and thus exhibit interesting onion-structured (or OS for short, or fullerene-structured, fullerene-like, *etc.*) nanoparticles (NPs),[10–15] which has attracted a special attention since the end of last century. It is well known that the structure of materials could determine their performances. The TMDC NPs with various structures would also bring many unique properties and applications,[16] including, but not limited to, the tribological applications, biomedicine, and electrical applications.

In early 1990s, the OS-WS_2 and OS-MoS_2 NPs were successively prepared by chemical reaction with the respective metal–oxide NPs in H_2S-contained reducing atmospheres at a quite high temperature (1000 °C).[13,14] Thereafter, research on OS-TMDC NPs began to enter people's vision. Several preparation methods have been developed for the OS-TMDC NPs including as-mentioned 'gas-solid' chemical reaction at high temperature,[13–15,17] thermal decomposition,[18,19] chemical vapor deposition (CVD),[20,21] laser fabrication (LF) in liquid or gas,[22–27] and so on.[28,29] Notably, all these methods need the high temperature environment, and involve chemical reaction of harmful substances (*e.g.* H_2S, sulfur) and time-consuming processes, except the LF processes, which are green, convenient, and scalable.[30,31] In addition, LF can produce extreme local environment (*e.g.* high temperature, high pressure) in a mild way (*e.g.* in liquid instantaneously), obtain good water–soluble nano-objects with tunable size, shape, defect state and phase composition by changing laser parameters (*e.g.* wavelength, frequency, pulse duration, power and time), target materials and media environment.[32] On these bases, LF has great potential in the preparation of OS-TMDC NPs. Here, we will mainly introduce the OS-TMDC especially the OS-MoS_2 NPs prepared by LF in liquids, and their performances and applications. Finally, a short outlook is also given.

2. OS-MoS_2 NPs

As a typical member of TMDCs, MoS_2 nanomaterials have especially attracted attention due to their specific physical and chemical properties,[33,34] so do the OS-MoS_2 NPs

[†]Corresponding author. E-mail: wpcai@issp.ac.cn

© 2022 Chinese Physical Society and IOP Publishing Ltd

prepared by LF. According to difference of dispersion media, the typical LF routes to those NPs can be divided into two categories: LF in gaseous environment and LF in liquid. In fact, the former usually refers to the laser ablation in gas (LAG), and the latter can also be subdivided into laser ablation in liquid (LAL) and laser irradiation in liquid (LIL). Figure 1 shows the illustrations of their experimental setups.

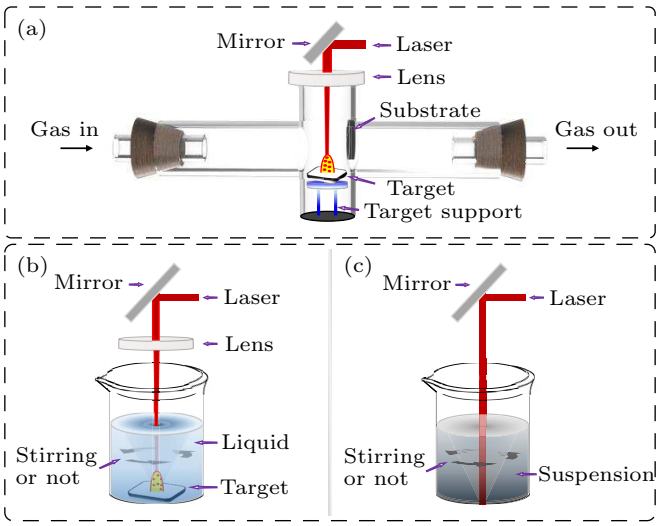


Fig. 1. The schematic illustrations of LF experimental setups: (a) LAG, (b) LAL, (c) LIL.

2.1. LAG

LAG was conducted by ablating a bulk target under protective atmosphere (or a precursor target under reactive atmosphere) via a focused pulse laser beam with specific parameters (Fig 1(a)). The laser beam with high energy would penetrate the target's surface within a certain depth, which depends on the laser parameters and the target materials, in a very short moment.[35] Then, the target in the irradiated area would absorb energy, produce local melting or plasma state, and eventually be expanded into the free space. Finally, the formed products could be transported by gas flow, deposited in a substrate, and collected. This process is called as LAG.[23,36]

In an early report, via laser ablation of a MoS_2 target under flowing He or Ar gas, Parilla *et al.*[22] first prepared nano-octahedral OS-MoS_2 NPs with size of 4–5 nm, which were once believed to represent the first 'inorganic fullerene', as shown in Figs. 2(a)–2(b). Also, Sen *et al.*[23] obtained the angular and hollow OS-MoS_2 NPs with $\sim$ 10 nm in size after laser ablation of MoS_2 target under Ar flow at 1050 °C (Fig. 2(c)), and found that their morphology and microstructure might be spherical with solid core if the temperature was lower. In fact, the products obtained in the LAG process were very complex, including roughly spherical, nested polyhedral, and tubular MoS_2 NPs, either crystalline or amorphous, as shown in Fig. 2(d).[10] Here, how to purify and separate was a problem worth considering. A theoretical simulation combining experiments reported by Bar-Sadan *et al.*[37] showed that small (< 2 nm) multiwall MoS_2 NPs with ideal octahedrons were unstable unless they were nonstoichiometric or over a limited size range of 10^4–10^5 atoms, beyond which they were converted into quasi-spherical multiwall MoS_2 NPs. More recently, Savva *et al.*[38] extended to prepare the OS-MoS_2 NPs with faceted shape, $\sim$ 100 nm in size and solid or hollow core (Fig. 2(e)) via ablation of MoS_2-Pb (molar ratio 1:1) mixed target in ambient air.

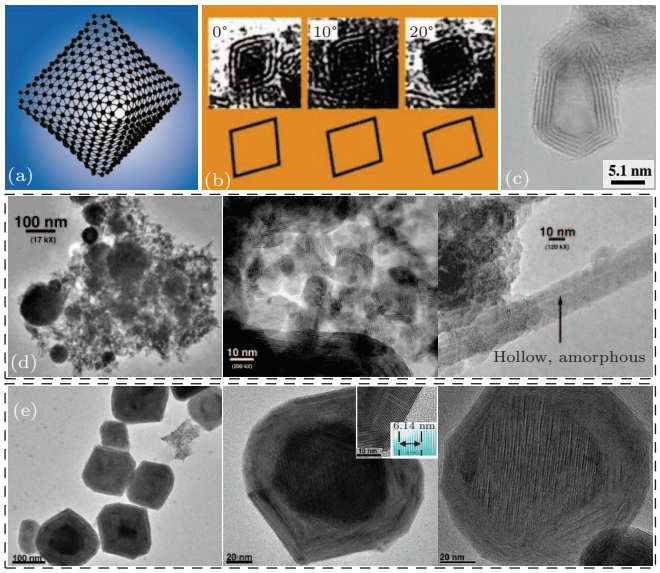


Fig. 2. Morphology and microstructure of the OS-MoS_2 NPs prepared by LAG. (a) A model of the octahedron built of Mo sublattice. (b) Transmission electron microscopy (TEM) images of OS-MoS_2 NPs in accord with model-generated projections for a three-layer MoS_2 rhomboid at different tilt angle.[22] Copyright 1999, Springer. (c) TEM image of the angular and hollow OS-MoS_2 NPs.[23] Copyright 2001, Elsevier. (d) TEM images of MoS_2 NPs with different shapes.[10] Copyright 2004, American Chemical Society. (e) TEM and high-resolution TEM (HRTEM) images of several typical OS-MoS_2 NPs prepared by LAG in ambient air.[38] Copyright 2017, American Chemical Society.

Alternatively, Song *et al.*[39] used laser to ablate a Mo target in dimethyl trisulfide (DMTS) gas that was carried by Ar gas, and obtained the pure OS-MoS_2 NPs, due to the laser-induced chemical reaction, as typically shown in Fig. 3(a). The similar OS-MoS_2 NPs could be also prepared by LAL via ablation of the Mo target in DMTS solution, but they were not pure OS-NPs, instead, there was a solid core inside, as illustrated in Fig. 3(b).

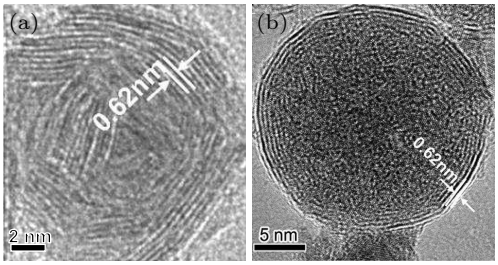


Fig. 3. HRTEM images of a typical MoS_2 NP prepared by laser ablation of an Mo target in different media.[39] (a) DMTS-contained atmosphere and (b) DMTS-contained solution. Copyright 2015, American Chemical Society.

Briefly, the OS-MoS_2 NPs with typical features such as the size ranging from several to hundreds of nanometers, the obvious faceted shape and solid or hollow core, could be prepared by LAG. However, such NPs seemingly always appeared together with their aggregations and other products of different shapes and composition, probably because the NPs formed during ablation process were easily agglomerated without effective dispersion. In addition, LAG method was usually cumbersome due to the complex gas circuit.

2.2. LAL

In addition to LAG method, LAL is the most common route to preparation of OS-MoS_2 NPs. Although the use of laser in LAL is the same as that in LAG (*e.g.* the focused pulse laser with controllable parameters), the LAL is much easier, as shown in Fig. 1(b). It just immerses a solid target in liquid (*e.g.* water, ethanol, and so on), rather than exposes it to the harsh and complex gas environments that are difficult to control. For LAL method, water was usually used as the main liquid. In a typical case, Wu *et al.*[24] first ablated MoS_2 target in water, and obtained the spherical MoS_2 NPs with single shape and about 120 nm in average diameter after filtering the colloidal products with 450-nm disposable filter, showing onion-like (or fullerene-like) structure, as shown in Fig. 4. Filter (also used in many other cases and will not mentioned repeatedly) could play an important role in the purification and separation of the OS-MoS_2 NPs from the as-prepared products with different shapes and sizes because the spherical NPs were usually small in size and not easy to filter out.

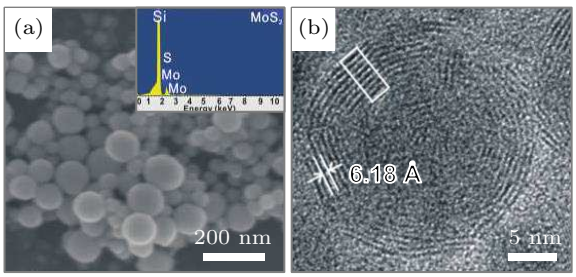


Fig. 4. The morphology of the OS-MoS_2 NPs prepared by LAL in water. (a) The SEM image of the products. The inset is the corresponding result of energy dispersive spectrum (EDS). (b) HRTEM image of a single NP.[24] Copyright 2011, American Chemical Society.

Subsequently, Compagnini *et al.*[25] found out that some of the OS-MoS_2 NPs prepared by the same LAL process in water had a solid core inside (as labelled with letter A in Fig. 5(a)), and that there existed MoO_3 NPs in products in addition to the OS-MoS_2 NPs, as labelled with letter B in Fig. 5(a). Such MoO_3 NPs could be closely related to the formation of the OS-MoS_2 NPs,[25] which would be described later. Moreover, the OS-MoS_2 NPs in the products would show different shapes, as shown in Fig. 5(b).

Zhou *et al.*[26] reported the laser ablation of MoS_2 target in water, and found that the obtained products consisted mostly of spherical NPs with very smooth surface and a large size dispersivity from tens to hundreds of nanometers in diameter, together with a few interesting tadpole-like long-tailed NPs, as shown in Fig. 6(a) and its inset. All products are MoS_2 NPs, in which the spherical NPs were onion-structured or concentrically built of nearly spherical {002} planes, whereas the tadpole-like MoS_2 NPs were built of cylindrically curved {002} planes, as shown in Figs. 6(b)–6(d). Also, there existed a big void and/or the dispersed porosities within the NPs. The porosity was estimated to be about 1%. The similar spherical OS-MoS_2 NPs with smooth surface were also reported by Chen *et al.*[27] and Compagnini *et al.*[25] using LAL in water with oscillation, although there existed slight surface oxidation.

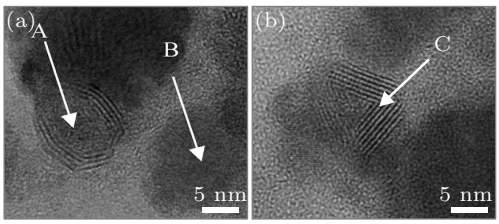


Fig. 5. The HRTEM images of the products obtained by laser ablation of MoS_2 in water.[25] The labels A and B refer to the OS-MoS_2 NP with solid core and the MoO_3 NP, respectively. The label C refers to the hollow OS-MoS_2 NP. Copyright 2014, Elsevier.

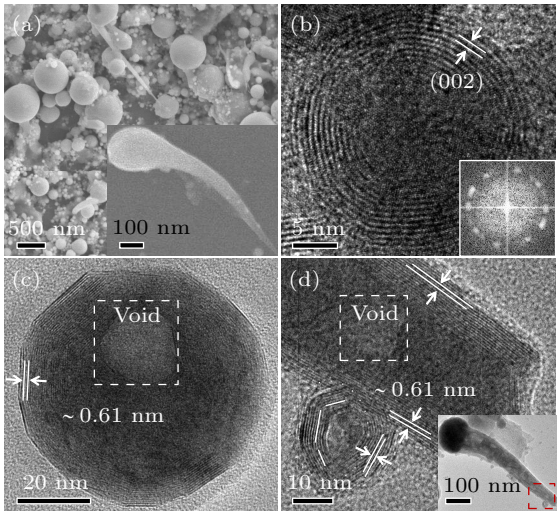


Fig. 6. The microstructural characterization of Zhou *et al.* prepared products by laser ablation of MoS_2 target in water.[26] (a) SEM image. The inset: the SEM image of a tadpole-like long-tailed NPs. (b)–(d) HRTEM images of some typical single OS-MoS_2 NPs. The insets in panels (b) and (d) are the corresponding Fourier transformation pattern and TEM image of the tadpole-like NPs with low magnification, respectively. Copyright 2017, American Chemical Society.

In terms of the laser-induced products, various experimental conditions would significantly affect their final morphology and structure.[40] However, for the specific OS-MX_2, the laser power and the dispersion media are the main factors that affect their formation. In the above examples, the laser power used was larger than ten micro Joules (mJ) per pulse during ablation of the MoS_2 target in water. If the power

was significantly reduced (around or below 0.1 mJ), the situation would be quite different. For instance, Ou *et al.*[41] and Sunitha *et al.*[42] used such laser power to ablate MoS_2 bulk target in water and obtained MoS_2 quantum dots (QDs) with size from 1.7 nm to 2.6 nm. Notably, these MoS_2 QDs did not exhibit onion-like structure. In addition to well-distributed S and Mo, O could be detected in the QDs, as shown in Fig. 7.

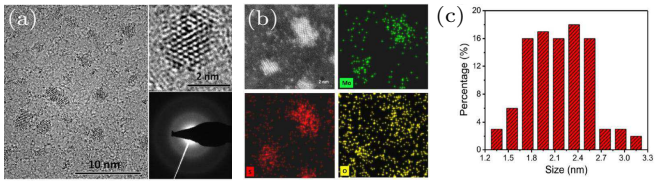


Fig. 7. Characterizations of MoS_2 QDs prepared by LAL in water with low laser power.[41] (a) HRTEM image, (b) EDS mapping, and (c) size distribution. The upper-right and lower-right insets in panel (a) are enlarged high-angle annular dark-field scanning TEM (HAADF-STEM) image and selected area electron diffraction (SAED) pattern, respectively. Copyright 2018, Springer.

In addition to water, some other liquids (such as surfactant-contained solution or organic solvent) were also be used. In order to improve the dispersion of the products, Han *et al.*[43] ablated MoS_2 bulk target in polyvinylpyrrolidone (PVP)-contained aqueous solution, and also obtained spherical OS-MoS_2 NPs, as typically illustrated Fig. 8. If the MoS_2 target in the ethylene glycol solution was ablated, however, the polyhedral and equal-axial MoS_2 NPs with the normal crystal structure were obtained and no onion-structured NP was formed.[44]

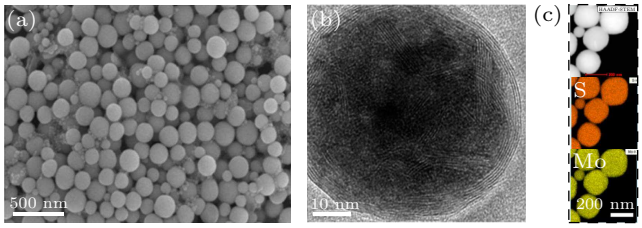


Fig. 8. Characterizations of MoS_2 NPs prepared by LAL in PVP-contained solution.[43] (a) SEM image of the products. (b) HRTEM image of single NP. (c) EDS elemental mapping of NPs. Copyright 2017, American Chemical Society.

2.3. LIL

LIL is another route of using laser to prepare NPs in liquid. Typically, the pre-prepared fine powders are first dispersed in liquid and then irradiated by an unfocused laser as illustrated in Fig. 1(c). Such route could induce the photothermal reduction effect in some cases, depending on the target material and the solution composition.[45–47] The dispersed powders can absorb laser energy when irradiated, which can selectively heat NPs in the liquid.[30,48] Thus, the powders would undergo fragmentation or melting process, and eventually be transformed into NPs. Typically, Alexaki *et al.*[49] irradiated MoS_2 platelets in aqueous solution and found that the as-prepared products could evolve with irradiation time in the size, shape, and composition (Fig. 9(a)). A relatively long irradiation time (*e.g.* 1000 s or longer) could make the MoS_2 platelets change to the spherical particles, in which there were a small number of the OS-MoS_2 NPs (Fig. 9(b)) but the rest were MoS_x (such as Mo_2S_3, *etc.*) NPs. Alternatively, Oztas *et al.*[50] used laser to irradiate MoS_2 powders in methanol. The products consist of the 2D thin MoS_2 nanosheets with 2 μm–3 μm in planar size, and the sub-micron spherical MoS_2 particles that exhibited onion-like structure, as shown in Fig. 9(c). However, Baldovi *et al.*[51] irradiated the commercial MoS_2 powders in acetonitrile and obtained spherical MoS_2 QDs (Fig. 9(d)) which were not onion-structured. In short, the formation of the OS-MoS_2 NPs via LIL depends on the irradiation conditions (the laser energy, irradiated time, liquid species, *etc.*). As for the nanosheets, they should originate from the exfoliation from the powder-targets due to laser-induced thermal shock as usually expected.

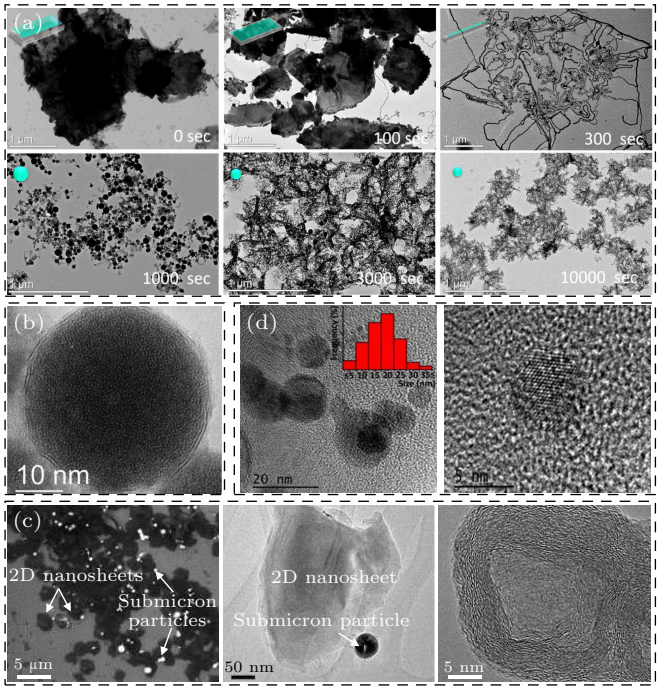


Fig. 9. Characterizations of the products prepared by laser irradiation of MoS_2 powderds in liquids. (a) TEM images for the morphological evolution of the products with the irradiation time during LIL, and (b) the HRTEM image of a typical spherical OS-MoS_2 NP.[49] Copyright 2018, American Chemical Society. (c) The TEM and HRTEM images of the MoS_2 NPs prepared by LIL in methanol.[50] Copyright 2014, American Chemical Society. (d) The HRTEM images of MoS_2 QDs obtained by LIL with low and high magnifications, and the inset is the size distribution.[51] Copyright 2016, Springer.

Totally, OS-MoS_2 NPs could be produced by LAL or LIL or LAG of MoS_2 targets. Laser energy, ablation/irradiation time, and medium species are important to the final products in structure and morphology, and the relatively low laser power is unbeneficial to generation of OS-TMDC NPs. Comparatively, LAL-based route could induce the complete spherical OS-TMDC NPs, while the LAG or LIL-based route mostly

produces the incomplete OS-TMDC NPs with non-spherical shapes and solid or hollow cores.

3. Other OS-TMDC NPs

In addition to OS-MoS_2 NPs, some other OS-TMDC NPs, such as OS-$MoSe_2$ NPs, OS-WS_2 NPs, *etc.*, could also be fabricated by the laser technology.

3.1. OS-$MoSe_2$ NPs

The faceted OS-$MoSe_2$ NPs with several nanometers in size could be prepared based on LAG via ablating $MoSe_2$ target, as shown in Figs. 10(a) and 10(b).[10,37] In contrast, via ablating $MoSe_2$ target in 30 vol% ethanol/water mixed solution, Wu *et al.*[52] obtained well-dispersed spherical OS-$MoSe_2$ NPs built of the concentrically spherical {002} planes of ~ 0.656 nm in spacing (Fig. 10(c)).

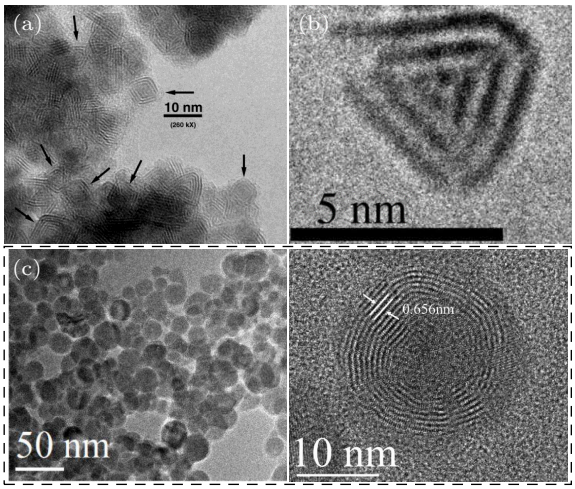


Fig. 10. Characterizations of OS-$MoSe_2$ NPs prepared by LF. (a) and (b) The HRTEM images of OS-$MoSe_2$ NPs prepared by LAG.[10,37] Copyright 2004 & 2006, American Chemical Society. (c) TEM and HRTEM images of the OS-$MoSe_2$ NPs prepared by LAL.[52] Copyright 2018, IOP Publishing.

3.2. OS-WS_2 NPs

Similarly, the laser-induced OS-WS_2 NPs have also attracted attention for a long time. In 2001, Sen *et al.*[23] found that a spherical OS-WS_2 NPs could be obtained by LAG of a WS_2 target at the relatively low temperature (below 700 °C) (Figs. 11(a) and 11(b)), and the hollow faceted and even tube-like OS-WS_2 NPs at a higher temperature ($\geq$ 850 °C) (Figs. 11(c) and 11(d)). Savva *et al.*[38] also reported the tube-like OS-WS_2 NPs via LAG of WS_2-Pb (molar ratio 1:1) mixed target in ambient air, and pointed out that some of the OS-WS_2 NPs were hollow whereas the rest exhibited an filled core, as shown in Fig. 11(e). In addition, Luo *et al.*[48] found that the smooth and solid spherical WS_2 NPs could be formed via LIL of WS_2 bulk-slice in ethanol, and exhibit the onion-structure, as shown in Figs. 11(f) and 11(g).

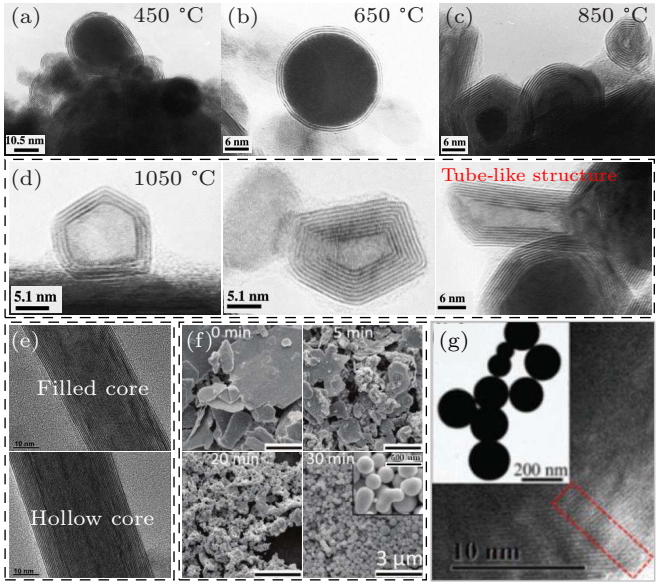


Fig. 11. The morphology and microstructure of the WS_2 NPs prepared by LF. (a)–(d) The HRTEM images of the typical OS-WS_2 NPs prepared by LAG of WS_2 bulk target at different temperatures.[23] Copyright 2001, Elsevier. (e) HRTEM images of the WS_2 NPs prepared by LAG of WS_2-Pb mixed target in ambient air.[38] Copyright 2017, American Chemical Society. (f) The morphological evolution of commercial WS_2 powders in ethanol during LIL (the inset is a magnified image) and (g) the HRTEM image of a WS_2 NP prepared by LIL, the inset is the SEM image of the LIL-induced products.[48] Copyright 2016, The Royal Society of Chemistry.

3.3. Others

Further, some other OS-TMDC NPs could also be successfully prepared via LF method. For instance, Schuffenhauer *et al.*[53] obtained the OS-TaS_2 NPs by both LAG and LAL methods, as typically shown in Fig. 12(a). Newly emerging OS-$NbSe_2$ and OS-SnS_2 NPs could also prepared via LAG

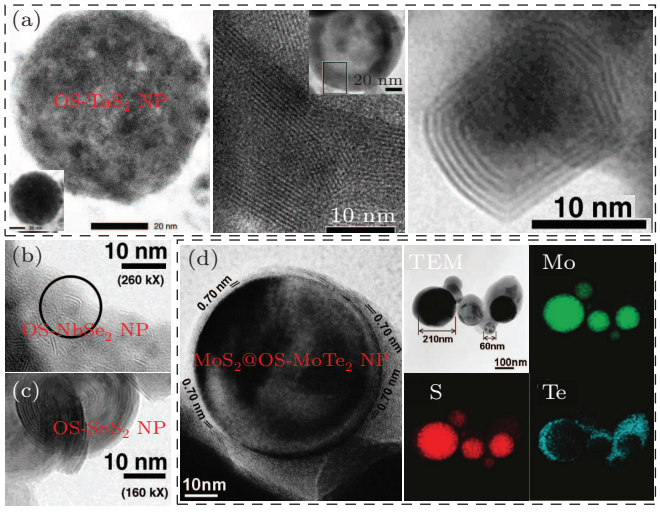


Fig. 12. The microstructural examinations of the laser-induced OS-NPs. (a) The HRTEM images of the typical OS-TaS_2 NPs prepared by different methods. Left: LAG of TaS_2-sulfur (molar ratio 1:100) mixed target in Ar. Middle: ablation of a TaS_2 target in liquid CS_2.[53] Copyright 2005, Wiley. Right: LAG of a TaS_2 target in Ar.[10] Copyright 2004, American Chemical Society. (b) and (c) The HRTEM images of (b) OS-$NbSe_2$ and (c) OS-SnS_2 NPs prepared by LAG in Ar.[10] Copyright 2004, American Chemical Society. (d) The HRTEM image and EDS mapping of MoS_2@OS-$MoTe_2$ NPs prepared by LAG of the MoS_2-Te mixed target.[54] Copyright 2008, American Chemical Society.

of corresponding bulk target in Ar, as given in Figs. 12(b) and 12(c).[10] Besides, MoS_2@OS-$MoTe_2$ core@shell composite NPs (Fig. 12(d)) were obtained.[54] All in all, LF has great potential in the preparation of various, but not limited to OS-TMDC NPs.

4. Formation mechanism

For the laser-induced OS-TMDC NPs mentioned above, there are several models to describe the formation of the laser-induced OS-TMDC NPs, including the template deposition growth, chemical reaction conversion, self-scrolling, fragmentation, and reshaping process, and liquid droplets' radial solidification/oriented growth, which depend on the specific LF routes.

4.1. Template deposition growth

The template deposition growth mechanism appears mainly in LAG cases. The OS-TMDC NPs prepared by LAG method mostly exhibited solid cores and onion-structure shells. Regardless of their size or shape (spherical, polyhedral or tube-like), the core parts of the NPs are always completely wrapped by the onion-structured shells (see Figs. 2(d) and 2(e), or Figs. 11(a)–11(e)), indicating a the inside-out growth mechanism.[23,38] Consequently, a mechanism of template deposition growth was proposed, or the inner cores serve as templates or supports, and the shells are formed via subsequent layer-by-layer deposition upon the cores during laser ablation, leading to the OS-TMDC NPs with solid cores. However, such mechanism cannot explain the hollow OS-TMDC NPs. In this regard, Sen *et al.*[23] claimed that the hollow NPs are usually polyhedral in profile, small in size and of few layers in shells. The hollow OS NPs were thus attributed to the curling of the ultrathin layer-structured nanosheets, since such nanosheets are favor of curling and closing themselves to form hollow NPs without help of core templates.

4.2. Chemical reaction conversion

The formation of some OS-TMDC NPs via LAG involves obvious chemical reaction processes. Typically, Song *et al.*[39] prepared the OS-MoS_2 NPs via ablating Mo target in DMTS gas,and proposed a possible reaction mechanism, as shown in Fig. 13. First, the laser shot induced molting at the local ablated area on the Mo target and form Mo nanodroplets (primary products), which would be ejected from the target surface under laser shot. Subsequently, before cooling, the nanodroplets would react, layer-by-layer from outside to inside, with the ambient medium, which depends on the cooling rate, laser power, and gas reactivity. The OS-MoS_2 NPs would thus be produced at low cooling rate, enough high laser power and high gas reactivity which could ensure the complete diffusion of S atoms and surface reaction (route 1). Otherwise, the low laser power or high cooling rate (*e.g.* laser ablation in DMTS liquid) would lead to incomplete surface reaction, resulting in the imcomplete OS-MoS_2 NPs (route 2) or the OS-MoS_2 NPs with solid core inside (route 3).

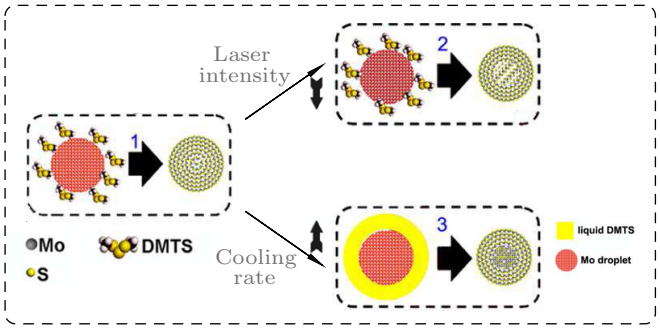


Fig. 13. Schematic illustration for the formation of the laser-induced OS-MoS_2 NPs (the details are seen in the text).[39] Copyright 2015, American Chemical Society.

Additionally, for the OS-MoS_2 NPs induced by direct ablation of MoS_2 target in water, Compagnini *et al.*[25] also proposed a mechanism of chemical reaction conversion, which was probably based on the OS-TMDC NPs obtained from 'gas–solid' chemical reaction at high temperature.[55,56] When direct ablation of MoS_2 target in water was carried out, Mo, S, and O, *etc.* would be produced in water due to the laser-induced plasma plume on the target, and hence MoO_3 and/or MoO_{3-x} NPs could inevitably be formed, while the formation of the molybdenum oxide is crucial to the subsequent formation of OS-MoS_2 because MoS_2 could be produced from the chemical reaction of molybdenum oxides with S at high temperature, or

$$MoO_3 + x/2S \rightarrow MoO_{3-x} + x/2SO_2\uparrow, \quad (1)$$

$$MoO_{3-x} + (7-x)/2S \rightarrow MoS_2 + (3-x)/2SO_2\uparrow. \quad (2)$$

The formed MoO_3 NPs would react with S to produce MoO_{3-x} (Eq. (1)), which could be transformed into MoS_2 via further reaction with S (Eq. (2)). Firstly, the reaction occurred on the surface of the oxide NPs to form 1–2 closed layers of MoS_2 shell, and then the S atoms diffused through the outer shells into the inner oxide cores. The OS-MoS_2 NPs were thus formed in such a way. The further experiments confirmed that if laser ablation was carried out in an oxygen-free environment (say, in n-decane), no OS-MoS_2 NPs could be obtained, indicating the importance of the oxidation environment in the formation of OS-MoS_2 NPs during the direct ablation of MoS_2 target.

4.3. Self-scrolling

It is conceivable that the onion-like structure could also result from the self-scrolling of nanosheets, which has been experimentally observed.[57,58] Typically, Oztas *et al.*[50]

found that a perfect MoS_2 nanosheet could not deform or deviate from the layer structure. However, if the nanosheets contain some vacancies (say, S defects), the deformation or self-scrolling would occur, especially when dispersed in water (or laser-ablated in water), leading to the formation of OS NPs. Obviously, such self-scrolling mechanism can well describe the formation of some tubular OS-TMDC NPs, but is not suitable for the spherical ones due to the geometric limitation.

4.4. laser-induced fragmentation and reshaping mechanism

Luo *et al.*[48] proposed the formation mechanism of the laser-induced fragmentation and reshaping for the LIL-induced OS-WS_2 NPs (Fig. 11(f)). The spherical OS-WS_2 NPs should be formed mainly through two steps, or the laser fragmentation and reshaping process. The original WS_2 slices would first explode into small fragments with irregular shape under laser shock (process I in Fig. 14). Subsequently, the pulsed-laser irradiation could cause heating, surface melting and rapid cooling of the small WS_2 fragments, which lead to the spheroidization and form spherical WS_2 NPs (process II–IV in Fig. 14). However, this mechanism can not explain the formation of the onion-like structure, which needs to take more details into consideration as follows.

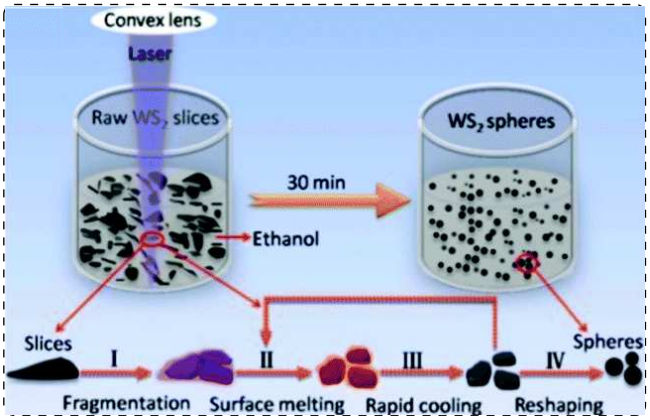


Fig. 14. Schematically illustration of the laser-induced fragmentation and reshaping mechanism for the LIL-induced spherical WS_2 NPs.[48] Copyright 2016, The Royal Society of Chemistry.

4.5. Laser-induced liquid droplets' radial solidification/oriented growth

Recently, Zhou *et al.*[26] has presented a mechanism based on laser-induced liquid droplets' radial solidification/oriented growth, which can well describe the formation of the LAL/LIL-induced OS-MoS_2 NPs with smooth surface. Briefly, the laser ablation of the MoS_2 target in water induced the local melting on the target and formed MoS_2 droplets. Such droplets would be ejected into water by the following laser shot, as shown in Fig. 15(a). Subsequently, the droplets would mostly assume the spherical shape due to the surface tension, before solidification in water. When the temperature in surface layer of the droplets was decreased below the melting point, MoS_2 nuclei would be formed randomly in the surface layer, as shown in Fig. 15(b). The MoS_2 nuclei should preferentially grow along {002} planes due to their crystal structure. So, only the nuclei, in which {002} plane is parallel to the surface tangent plane of the droplet, could grow along {002} plane till contact with the neighbouring growing nuclei and solidification of surface layer of the droplet, as shown in Fig. 15(c). After the surface-layer of the droplet was solidified, the radial solidification began and led to the inward {002}-oriented growth, due to the radial heat-dissipation of the droplet, as shown in Fig. 15(d). As the inward growth was going on, the melten MoS_2 was continuously consumed. Finally, the spherical OS-MoS_2 NPs, which were built of concentrically spherical {002} planes, were formed with a void in the core part, as shown in Figs. 15(e) and 15(f). Due to the density difference between solid and liquid of MoS_2, there exist the volume shrinkage and/or the porosities in the central part of the droplet, as shown in Figs. 6(c) and 6(d) or Figs. 15(e) and 15(f). The solidification contraction for MoS_2 is about 1%–2.5%, which is in agreement with the observation.[26]

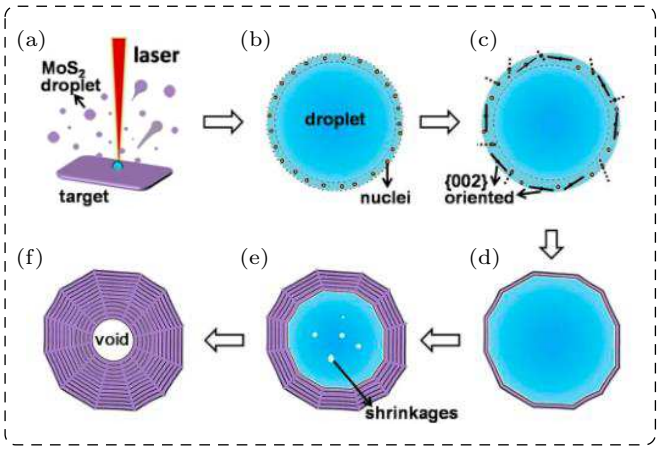


Fig. 15. Schematic illustration of laser-induced liquid droplets' radial solidification/oriented growth mechanism for the OS-MoS_2 NPs (the details are seen in the text).[26] Copyright 2017, American Chemical Society.

As for the tadpole-like NPs shown in Figs. 6(a) and 6(d), they were attributed to the reason that the surface solidification of the liquid droplets ejected from the target surface into water took place before surface tension-induced formation of spherical droplet. Similarly, for such tadpole-like droplet, the cylindrical {002} planes were formed in the surface layer of the droplet, during surface solidification. With inward radial solidification, the tadpole-like NPs were thus formed and built of concentrically cylindrical {002} crystal planes with one void or several holes inside due to the volume contraction, as typically shown in Fig. 16.

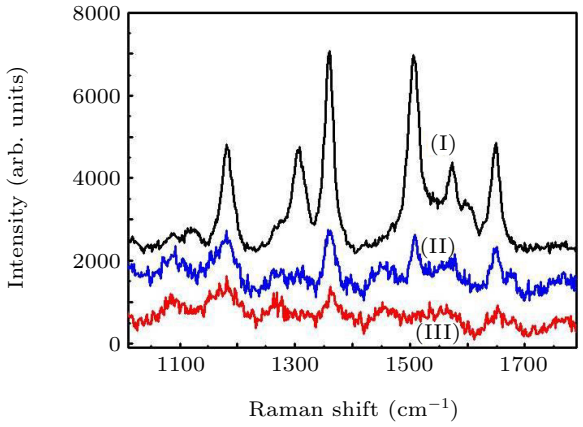


Fig. 16. Raman spectra of R6G molecules on virous substrates including (I) spherical OS-MoS_2 NPs-built film, (II) MoS_2 nanosheets-built film, and (III) blank silicon wafer.[26] Copyright 2017, American Chemical Society.

5. Properties and applications

As mentioned above, the OS-TMDC NPs have many applications in such as tribological and impact resistance, tips for scanning-probe microscopy, and so on.[16] Here we briefly introduce some special properties or applications of the laser-induced OS-TMDC NPs.

5.1. Good biocompatibility

The OS-TMDC NPs prepared by LAL in water have good water-solubility. In cell viability experiment, Wu *et al.*[24] found that such OS-MoS_2 NPs were nontoxic to the various cells (*e.g.* human embryonic epidermal fibroblast cells, lung adenocarcinoma cells, and leukemic cells) at a given concentration, indicating various potential biomedical applications.

5.2. Structure-Enhanced surface-enhanced Raman scattering (SERS) effect

MoS_2 nanomaterials possess SERS effect to Rhodamine 6G (R6G) molecules due to the charge transfer-induced chemical enhancement mechanism.[59,60] Zhou *et al.*[26] found that the OS-MoS_2 NPs-built film could exhibit significantly higher Raman signals than those of MoS_2 nanosheets-built film (or black silicon), as shown in Fig. 16. Such enhancement was attributed to the special structure of the spherical OS-MoS_2 NPs, which could enhance the charge transfer ability between R6G molecules and MoS_2.[61] In addition, the stacked spherical OS-MoS_2 NPs have the higher exposed surface area than that of the stacked MoS_2 nanosheets which are easily overlapped, leading to better SERS effect.

5.3. Tribological application

Chen *et al.*[27] reported that the OS-MoS_2 NPs, added in hyaluronic acid (HA)-based artificial synovial fluid, were the efficient friction reducers and could improve tribological behavior. This could be attributed to the bearing effect and protective-film effect. On one hand, the spherical OS-MoS_2 NPs dispersed in HA synovial fluid can work as ball bearings, leading to rolling friction at the friction interface. In addition, sliding may occur between external curved planes of the OS-MoS_2 NP and contribute to low friction because of the weak interaction (van der Waals force) between adjacent layers. On the other hand, the OS-MoS_2 NPs is spherically closed structure without dangling bonds, which can also become a protective film which help forming a highly ordered bending structure to cover the rough friction surface.

6. Summary and outlook

In summary, we have given a brief introduction of the laser-induced OS-TMDC NPs (especially for OS-MoS_2 NPs), including their different preparation routes, formation mechanism, properties, and applications. In preparation, LAL and LIL provide the more common and flexible routes to the OS-TMDC NPs than LAG. The various mechanisms have been introduced based on different preparation routes, including the template deposition growth, the chemical reaction conversion, the self-scrolling, the laser-induced fragmentation and reshaping, and the laser-induced liquid droplets' radial solidification/oriented growth, which can describe the formations of the corresponding OS-NPs. Finally, some interesting properties and novel applications of these NPs are briefly demonstrated.

Of course, there are some unsolved problems that are worth deep-studying. For example, is it hardly to obtain OS-TMDC NPs by LF in organic liquids? It is obvious that there is a critical laser power or intensity for the formation of such OS-TMDC NPs, but how to determine it? How to achieve the mass-production of such OS-NPs? Future researches could include but are not limited to these aspects. In addition, OS-TMDC composite NPs are also worth more studying based on LF methods, which could bring new performances and applications.

Acknowledgments

Project supported by the National Key Research and Development Program of China (Grant No. 2017YFA0207101) and the National Natural Science Foundation of China (Grant Nos. 11974352 and 51771182).

References

[1] Wang Q H, Kalantar-Zadeh K, Kis A, Coleman J N and Strano M S 2012 *Nat. Nanotechnol.* **7** 699
[2] Manzeli S, Ovchinnikov D, Pasquier D, Yazyev O V and Kis A 2017 *Nat. Rev. Mater.* **2** 17033
[3] Liu W J, Liu M L, Wang X T, Shen T, Chang G Q, Lei M, Deng H X, Wei Z M and Wei Z Y 2019 *ACS Appl. Nano Mater.* **2** 2697
[4] Mattinen M, Leskela M and Ritala M 2021 *Adv. Mater. Interfaces* **8** 2001677
[5] Meng Z, Stolz R M, Mendecki L and Mirica K A 2019 *Chem. Rev.* **119** 478

[6] Zhou X, Sun H and Bai X 2020 *Front. Bioeng. Biotechnol.* **8** 236
[7] Bai J, Zhao B, Wang X, Ma H, Li K, Fang Z, Li H, Dai J, Zhu X and Sun Y 2020 *J. Power Sources* **465** 228282
[8] Zhou L, Zhang H, Bao H, Wei Y, Fu H and Cai W 2020 *ACS Appl. Nano Mater.* **3** 624
[9] Chen M, Lin Z, Xuan M, Lin X, Yang M, Dai L and He Q 2021 *Angew. Chem. Int. Ed.* **60** 16674
[10] Parilla P A, Dillon A C, Parkinson B A, Jones K M, Alleman J, Riker G, Ginley D S and Heben M J 2004 *J. Phys. Chem. B* **108** 6197
[11] Feldman Y, Zak A, Popovitz-Biro R and Tenne R 2000 *Solid State Sci.* **2** 663
[12] Rapoport L, Fleischer N and Tenne R 2005 *J. Mater. Chem.* **15** 1782
[13] Tenne R, Margulis L, Genut M and Hodes G 1992 *Nature* **360** 444
[14] Margulis L, Salitra G, Tenne R and Talianker M 1993 *Nature* **365** 113
[15] Rosentsveig R, Margolin A, Gorodnev A, Popovitz-Biro R, Feldman Y, Rapoport L, Novema Y, Naveh G and Tenne R 2009 *J. Mater. Chem.* **19** 4368
[16] Tenne R 2006 *J. Mater. Res.* **21** 2726
[17] Yadgarov L, Choi C L, Sedova A, Cohen A, Rosentsveig R, Bar-Elli O, Oron D, Dai H J and Tenne R 2014 *ACS Nano* **8** 3575
[18] Nath M, Govindaraj A and Rao C N R 2001 *Adv. Mater.* **13** 283
[19] Chen J, Li S L, Gao F and Tao Z L 2003 *Chem. Mater.* **15** 1012
[20] Li X L, Ge J P and Li Y D 2004 *Chem. Eur. J.* **10** 6163
[21] Etzkorn J, Therese H A, Rocker F, Zink N, Kolb U and Tremel W 2005 *Adv. Mater.* **17** 2372
[22] Parilla P A, Dillon A C, Jones K M, Riker G, Schulz D L, Ginley D S and Heben M J 1999 *Nature* **397** 114
[23] Sen R, Govindaraj A, Suenaga K, Suzuki S, Kataura H, Iijima S and Achiba Y 2001 *Chem. Phys. Lett.* **340** 242
[24] Wu H H, Yang R, Song B M, Han Q S, Li J Y, Zhang Y, Fang Y, Tenne R and Wang C 2011 *ACS Nano* **5** 1276
[25] Compagnini G, Sinatra M G, Messina G C, Patane G, Scalese S and Puglisi O 2012 *Appl. Surf. Sci.* **258** 5672
[26] Zhou L, Zhang H, Bao H, Liu G, Li Y and Cai W 2017 *J. Phys. Chem. C* **121** 23233
[27] Chen T, Zou H, Wu X, Chen Y, Bo S, Zheng L and Yang G 2019 *ACS Biomater. Sci. Eng.* **5** 3079
[28] Hsu W K, Chang B H, Zhu Y Q, Han W Q, Terrones H, Terrones M, Grobert N, Cheetham A K, Kroto H W and Walton D R M 2000 *J. Am. Chem. Soc.* **122** 10155
[29] Vollath D and Szabo D V 2000 *Acta Mater.* **48** 953
[30] Zhang D S, Goekce B and Barcikowski S 2017 *Chem. Rev.* **117** 3990
[31] Liu Le, Xu L, Zhang H and Chen M 2017 *Chin. Phys. B* **26** 085206
[32] Ali N, Bashir S, Umm-i-Kalsoom, Rafique M S, Begum N, Husinsky W, Ajami A and Natahala C S R 2017 *Chin. Phys. B* **26** 015204
[33] Zhou L, Zhang H, Bao H, Liu G, Li Y and Cai W 2018 *J. Phys. Chem. C* **122** 8628
[34] Liu H, Su D, Zhou R, Sun B, Wang G and Qiao S Z 2012 *Adv. Energy Mater.* **2** 970
[35] Zeng H B, Du X W, Singh S C, Kulinich S A, Yang S K, He J P and Cai W P 2012 *Adv. Funct. Mater.* **22** 1333
[36] Hashida M, Mishima H, Tokita S and Sakabe S 2009 *Opt. Express* **17** 13116
[37] Bar-Sadan M, Enyashin A N, Gemming S, Popovitz-Biro R, Hong S Y, Prior Y, Tenne R and Seifert G 2006 *J. Phys. Chem. B* **110** 25399
[38] Savva K, Visic B, Popovitz-Biro R, Stratakis E and Tenne R 2017 *ACS Omega* **2** 2649
[39] Song S-T, Cui L, Yang J and Du X-W 2015 *ACS Appl. Mater. Interfaces* **7** 1949
[40] Liang C, Sasaki T, Shimizu Y and Koshizaki N 2004 *Chem. Phys. Lett.* **389** 58
[41] Ou G, Fan P X, Ke X X, Xu Y S, Huang K, Wei H H, Yu W, Zhang H J, Zhong M L, Wu H and Li Y D 2018 *Nano Res.* **11** 751
[42] Sunitha A P, Hajara P, Shaji M, Jayaraj M K and Saji K J 2018 *J. Lumin.* **203** 313
[43] Han Q, Cai S, Yang L, Wang X, Qi C, Yang R and Wang C 2017 *ACS Appl. Mater. Interfaces* **9** 21116
[44] Moniri S and Hantehzadeh M R 2021 *Opt. Quantum Electron.* **53** 215
[45] Song X, Qiu Z, Yang X, Gong H, Zheng S, Cao B, Wang H, Möhwald H and Shchukin D 2014 *Chem. Mater.* **26** 5113
[46] Luo T, Chen X, Li P, Wang P, Li C, Cao B, Luo J and Yang S 2018 *Nanotechnology* **29** 265704
[47] Luo T, Chen X, Wang P, Li C, Cao B and Zeng H 2018 *Adv. Mater. Interfaces* **5** 1700839
[48] Luo T, Wang P, Qiu Z, Yang S, Zeng H and Cao B 2016 *Chem. Commun.* **52** 10147
[49] Alexaki K, Kostopoulou A, Sygletou M, Kenanakis G and Stratakis E 2018 *ACS Omega* **3** 16728
[50] Oztas T, Sen H S, Durgun E and Ortac B 2014 *J. Phys. Chem. C* **118** 30120
[51] Baldovi H G, Latorre-Sanchez M, Esteve-Adell I, Khan A, Asiri A M, Kosa S A and Garcia H 2016 *J. Nanopart. Res.* **18** 240
[52] Wu X, Tian X, Chen T, Zeng A and Yang G 2018 *Nanotechnology* **29** 295604
[53] Schuffenhauer C, Parkinson B A, Jin-Phillipp N Y, Joly-Pottuz L, Martin J M, Popovitz-Biro R and Tenne R 2005 *Small* **1** 1100
[54] Hu J J, Zabinski J S, Bultman J E, Sanders J H and Voevodin A A 2008 *Cryst. Growth Des.* **8** 2603
[55] Zak A, Feldman Y, Alperovich V, Rosentsveig R and Tenne R 2000 *J. Am. Chem. Soc.* **122** 11108
[56] Weber T, Muijsers J C, vanWolput H, Verhagen C P J and Niemantsverdriet J W 1996 *J. Phys. Chem.* **100** 14144
[57] Seo J W, Jun Y W, Park S W, Nah H, Moon T, Park B, Kim J G, Kim Y J and Cheon J 2007 *Angew. Chem. Int. Ed.* **46** 8828
[58] Sharifi T, Gracia-Espino E, Barzegar H R, Jia X E, Nitze F, Hu G Z, Nordblad P, Tai C W and Wagberg T 2013 *Nat. Commun.* **4** 2319
[59] Sun L, Hu H, Zhan D, Yan J, Liu L, Teguh J S, Yeow E K, Lee P S and Shen Z 2014 *Small* **10** 1090
[60] Xu Y Y, Yang C, Jiang S Z, Man B Y, Liu M, Chen C S, Zhang C, Sun Z C, Qiu H W and Li H S 2015 *Appl. Surf. Sci.* **357** 1708
[61] Xu H, Xie L M, Zhang H L and Zhang J 2011 *ACS Nano* **5** 5338